Article ID: 1003－6326(2005)06－1226－05

Evaluation of pitting corrosion of Al-Mg-Mn-Sc-Zr alloy in EXCO solution by EIS①

PENG Yong-yi(彭勇宜)[1,2], YIN Zhi-min(尹志民)[2], LI San-hua(黎三华)[1]
(1. School of Physics Science and Technology, Central South University, Changsha 410083, China;
2. School of Materials Science and Engineering, Central South University, Changsha 410083, China)

Abstract: In order to evaluate the degree and severity of Al-Mg-Mn-Sc-Zr alloy in exfoliation corrosion(EXCO) solution quickly and nondestructively, electrochemical impedance spectroscopy(EIS) technique was employed. The Al-Mg-Mn-Sc-Zr alloy suffers pitting corrosion in the EXCO solution. During pit incubation, the Nyquist diagram is composed of a depressed capacitive arc at high-mediate frequency and an inductive arc at low frequency. The inductive arc fades with immersion time, and the beginning of pitting corrosion and the appearance of two capacitive arcs have simultaneity. During pit propagation, the Nyquist diagram is composed of two overlapped capacitive arcs. As time goes on, two time constants are more clearly distinguished. The high frequency and low frequency capacitive arc are aroused by passive surface and new interface, respectively. An equivalent circuit is designed to fit EIS, and the experimental results and the fitted results have good correspondence. The degree and severity of pitting corrosion can be obtained by the features of EIS and comparing the fitted values of parameters at different times.

Key words: Al-Mg-Mn-Sc-Zr alloy; EXCO solution; pitting corrosion; EIS
CLC number: TG 174.3 **Document code:** A

1 INTRODUCTION

Studies have shown that the Al-Mg alloy containing minor Sc and Zr has outstanding mechanical properties[1], weldability, fatigue fracture resistance and high-temperature stability[2,3]. The strength of Al-Mg-Mn alloy with Sc and Zr is much higher than that of Al-Mg-Mn alloy without Sc and Zr, and it will be a neotype and light-mass structural material used widely in warship, aerospace and aviation industries. However, in this alloy, β phase(Mg_5Al_8) precipitates easily along grain boundary, and the corrosion potential of β phase is much lower than that of matrix[4], which causes its sensitivity to corrosion. Then, the strength and plasticity decrease. This is very dangerous if the alloy is in the course of service. It is necessary to find a fast, reliable and nondestructive method to detect corrosion.

EIS technique just can be used to evaluate the severity of corrosion quickly, semi-quantitatively and nondestructively. Recently EIS technique has been used gradually in the study of corrosion[5-7], and some researchers have proposed theoretical model of corrosion[8-10]. EIS technique was also considered a powerful tool to investigate different stages of pitting corrosion.

The objective of this paper is to investigate the EIS of Al-Mg-Mn-Sc-Zr alloy during the different stages of pitting corrosion, and to attempt to disclose the relationships between severity of pitting corrosion and the features of EIS.

2 EXPERIMENTAL

2.1 Materials

The major composition (mass fraction, %) of the aluminum alloy is Mg 5.2, Mn 0.3, Sc 0.25, Zr 0.12, Al balance. The alloy ingot was produced by semi-continuous casting technique. The 3.4 mm-thick sheets were annealed for stabilization at 350 ℃ for 1 h in the end. Specimens were sawed from a large annealed sheet.

2.2 Experimental methods

The surface of specimens for this investigation was ground using abrasive papers from 600# to 1400#, polished with diamond paste, degreased using acetone, rinsed with distilled water and dried in air. The specimen for measurement of EIS was connected to a copper wire, and then mounted in epoxy resin with only 7 cm^2 surface exposed.

The accelerated exfoliation test was performed according to ASTM G66-80[11]. The exfoliation

① **Foundation item:** Project(G1999064911) supported by the National Basic Research Program of China
Received date: 2005－03－18; **Accepted date:** 2005－06－20
Correspondence: PENG Yong-yi, PhD candidate; Tel: +86-731-8836276; E-mail: pengyongyi@126.com

corrosion(EXCO) solution was prepared: dissolving 1 mol NH_4Cl, 0.25 mol NH_4NO_3, 0.01 mol $(NH_4)_2C_4H_2O$, 3 g H_2O_2(10 mL 30% stock solution) in distilled water and diluted to 1 L. The EXCO volume-to-exposed specimen surface area ratio was 80 mL/cm^2. The susceptibility to exfoliation was determined by visual examination using performance ratings established by reference to standard photographs.

Measurement of electrochemical impedance spectroscopy was carried out using the three electrode system of a saturated calomel reference electrode, a platinum counter electrode and a working electrode of the alloy being studied with about 7 cm^2 exposed surface. Three electrode cells were connected to a Solartron 1287 Potentiostat and a Solartron 1255B frequency response analyzer. A sinusoidal potential of 10 mV amplitude and a frequency sweep of 100 kHz to 0.005 Hz was used as disturbance signal during the measurement.

3 RESULTS AND DISSCUSSION

The specimens were immersed continuously in the EXCO solution for 48 h. The corrosion morphologies of specimens after different immersion time are shown in Fig. 1. And the corrosion degrees are listed in Table 1.

The typical Nyquist impedance spectroscopy at early immersion stage is shown in Fig. 2. The corresponding Bode diagram is shown in Fig. 3. It is clearly seen that the Nyquist diagram is mainly composed of a depressed capacitive arc at high-mediate frequency and an inductive loop at low frequency. The depressed capacitive arc is due to the surface roughness, which is accompanied by a distribution of relaxation times around the most probable value[12]. The relationship between depression of Nyquist diagram and surface roughness is even more evident in aluminium alloys[12]. On one hand, at the early stage of immersion, the corrosion process itself causes an increase in the surface irregularity of specimen; on the other hand, there are a lot of precipitates with different electrochemical natures due to the heat treatment of the alloys.

Table 1 Corrosion degree of specimens at different immersion times

Immersion time/h	10	17	24	36	48
Corrosion degree	PA	PB	≤PC	PC	> PC

PA, PB, PC: three degrees of pitting, PA< PB< PC[11]

Cao et al[13] thought that the inductive arc is linked to the passive film on the surface, and the appearance of inductive component is the feature of EIS during pit incubation. They analyzed the growth and decline of passive film during pit incubation, put forward a mathematical model and the corresponding equivalent circuit. The Nyquist diagram of the equivalent circuit is composed of a capacitive arc at high-mediate frequency and an inductive loop at low frequency. Keddam et al[14] thought that the inductive loop observed is associated with the weakening of the protective effectiveness of the aluminum oxide layer due to the anodic dissolution of aluminum alloy. Ferreira et al also

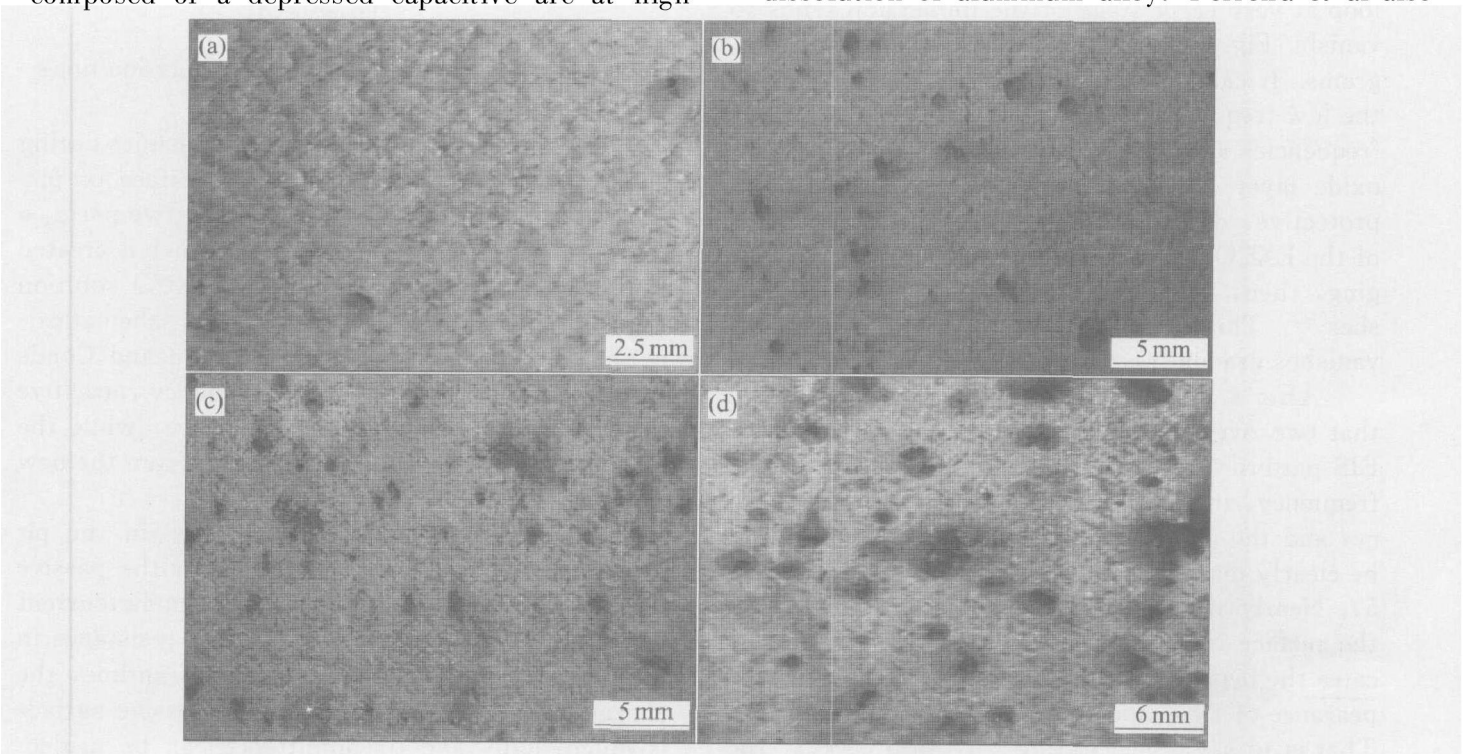

Fig. 1 Corrosion morphologies of specimens after different immersion times in EXCO solution
(a) —8.2 h; (b) —24 h; (c) —36 h; (d) —48 h

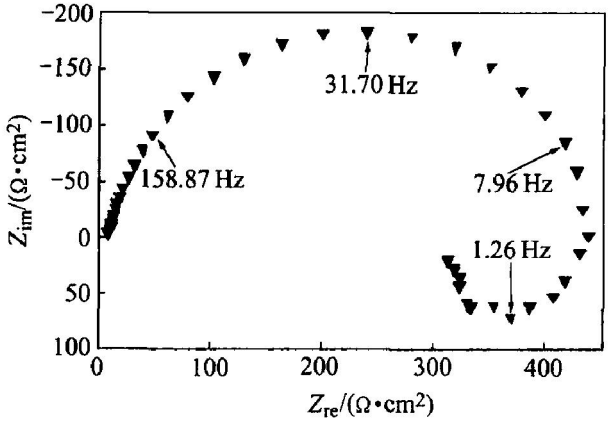

Fig. 2 Nyquist diagram after 3.5 h immersion

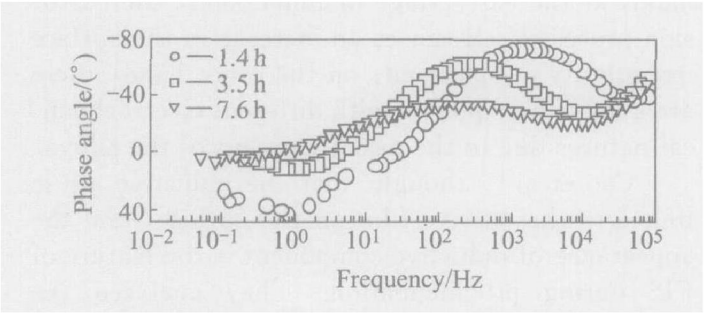

Fig. 3 Bode diagrams of specimens at different immersion time

observed an inductive loop in the early stage of pitting corrosion, and they put forward an equivalent circuit which contains negative resistance and negative capacitance to explain this phenomenon. But the physical meaning of negative resistance and negative capacitance is not definite.

With increasing immersion time, the inductive loop at very early stage of the immersion tends to vanish. Fig. 3 shows the evolution of Bode diagrams. It can be seen that, the inductive loop in the low-frequency range shifts with time to lower frequencies and disappears gradually. The surface oxide layer becomes progressively less and less protective, due to the action of aggressive anions of the EXCO solution with immersion time prolonging, then, the relaxation of weak points diminishes[14]. This can explain why the inductive loop vanishes gradually.

After 8.2 h of immersion, it is clearly found that two overlapped capacitive arcs appear on the EIS pattern (Fig. 4). One is in the high-mediate frequency, the other is in the mediate-low frequency, and the corresponding two time constants can be clearly distinguished in the Bode diagram (Fig. 5). Nearly at the same time, pits can be visible on the surface of specimens (Fig. 1(a)). This indicates the beginning of pitting corrosion and the appearance of two capacitive arcs have simultaneity. That is to say, once pitting corrosion occurs, the inductive arc disappears and two capacitive arcs appear on EIS pattern.

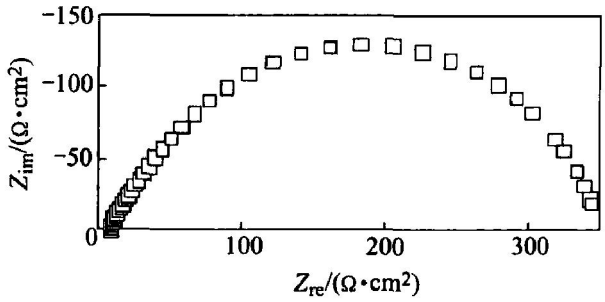

Fig. 4 Nyquist diagram after 8.2 h immersion

With prolonging the immersion time, two overlapped capacitive arcs become more clear in the Nyquist diagram, and the corresponding two time constants are revealed more clearly in the Bode diagram (Fig. 5). This can be seen from the reduction in the height and width of the maximum of the phase angle. The more clearly the two time constants can be distinguished, the greater the size and the number of the pits become. A similar behavior was reported by Conde et al[15]. They observed that when the surface of the specimen was covered by small pits, the impedance technique was not capable of detecting them until the area covered by pits is large enough.

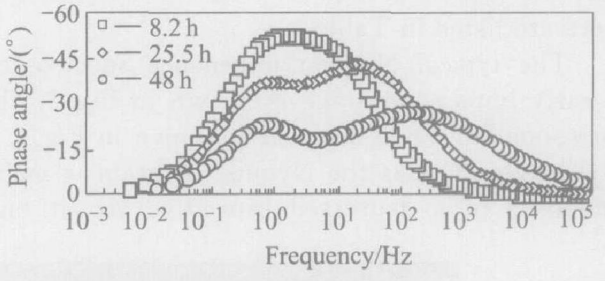

Fig. 5 Bode diagrams at different immersion times

According to electrochemical mechanics during pits propagation, the surface or interface of pitting-attacked specimen is composed of two parts: a passive surface and a new interface which is created by pitting-attack and exposure to EXCO solution through pits. This pitting structure is schematically shown in Fig. 6. Besides, Keddam and Conde thought that the high-mediate frequency capacitive arc originates from the passive surface, while the mediate-low frequency one originates from the new interface attacked by pitting corrosion.

During pit propagation, the area in the pit (anode region) is much smaller than the passive surface (cathode region), and the anodic current density is very high, so the solution resistance in the pit must be considered. In the meantime, the charge-transfer resistance from the passive surface is much high, and its admittance can be neglected[16]. On the basis of this concept, an equivalent circuit (shown in Fig. 7) is designed to fit the

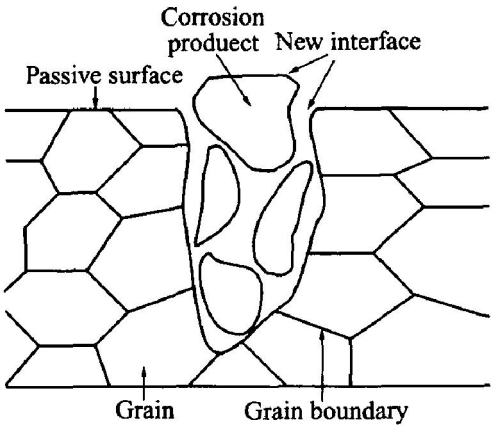

Fig. 6 Sketch of pitting surface

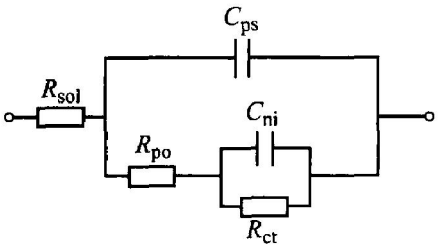

Fig. 7 Equivalent circuit used for fitting

impedance during pit propagation. In this equivalent circuit, the electrolyte resistance between reference electrode and working electrode is defined as R_{sol}, the double-layer capacitance corresponding to the passive surface and the new interface is represented by C_{ps} and C_{ni}, respectively, R_{po} is the electrolyte resistance inside the pore and R_{ct} is the charge-transfer resistance from the pore.

The experimental results of the impedance are fitted and analyzed in terms of equivalent circuit using Zview program. During the fitting, all the capacitances are replaced by constant-phase element (CPE) in order to consider the behaviors, which do not correspond, exactly, to pure capacitances. Then, the impedance of CPE is defined by the following equation: $Z_{CPE} = 1/[C(j\omega)^n]$, where C is a constant, ω is the angular frequency, n ranges between 0 and 1. As $n = 1$, Z_{CPE} represents an ideal capacitance; $n = 0$, a resistance; $n = -1$, a inductance; and $n = 0.5$, a Warburg impedance.

Table 2 lists the fitted results of the electrochemical impedance spectroscopy. The good correspondence between the experimental curves and the modeled curves is obtained using this equivalent circuit. The experimental and fitted impedance spectra after 12.3 h and 36 h immersion as examples are shown in Fig. 8.

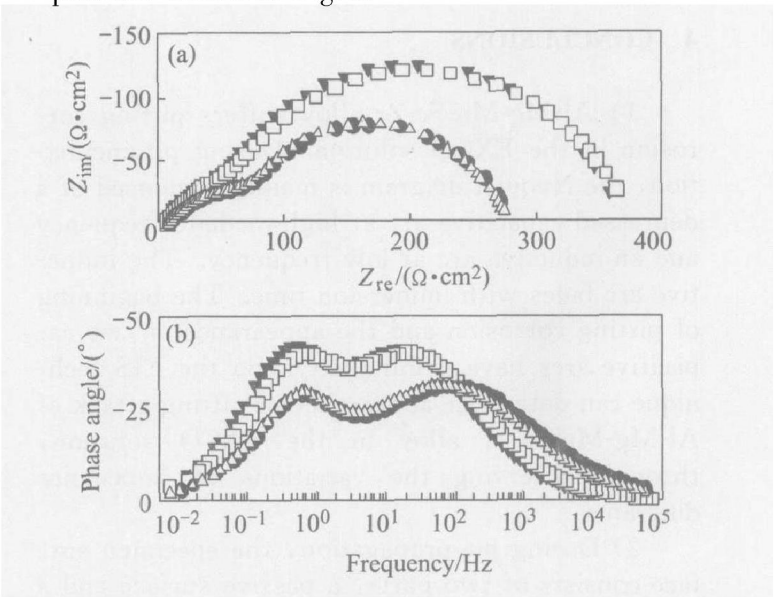

Fig. 8 Experimental and fitted impedance spectra after 12.3 h and 36 h immersion
(▼—12.3 h, experimental; □—12.3 h, fitted; ●—36 h experimental; △—36 h, fitted)

As shown in Table 2, R_{sol} is very low and can be neglected, R_{po} has tendency of increase and R_{po} is a parameter which reflects the depth of pore and the electric conductivity of solution in pore. If the electric conductivity of solution in pore is a constant, then the deeper the pore is, the higher the R_{po}. R_{ct} decreases gradually after immersion for 12.3 h, and this regularity is caused by the self-catalyzed reaction in the pore during pit propagation. C_{ps} decreases and C_{ni} increases with immersion time prolonging. This indicates the decrease of passive surface, the increase and growth of pit. Capacitance C is defined by the equation: $C = \varepsilon S/d$, where ε is dielectric constant, S is the area of surface, and d is the thickness of the film or the double-layer. Then, $C_{ps} = \varepsilon S_1/d_1$, $C_{ni} = \varepsilon S_2/d_2$. ε, ε can be regarded as the constant, and the change of S_1 and S_2 is greater than that of d_1 and d_2, therefore C_{ps} and C_{ni} are in direct proportion to the area of passive surface and new interface. That

Table 2 Fitted values of electrochemical impedance spectroscopy

Immersion time/h	R_{sol}/($\Omega \cdot cm^2$)	C_{ps}/(10^{-4} $\Omega^{-1} \cdot cm^{-2} \cdot s^{-n}$)	n_1	R_{po}/($\Omega \cdot cm^2$)	C_{ni}/(10^{-4} $\Omega^{-1} \cdot cm^{-2} \cdot s^{-n}$)	n_2	R_{ct}/($\Omega \cdot cm^2$)
8.2	7.85	16.896	0.847	91.82	15.250	0.868	250.2
12.3	6.92	13.672	0.715	89.04	20.694	0.917	267.6
25.5	6.54	10.784	0.722	102.50	23.943	0.897	191.5
36.0	8.17	9.245	0.568	104.60	27.539	0.910	170.0
48.0	10.38	7.610	0.541	109.20	29.583	0.933	130.9

is to say, the decrease of C_{ps} is caused by the decrease of the passive surface, and the increase of C_{ni} is caused by the increase of the new interface. This indicates that the value of C_{ni}/C_{ps} can also reflect the severity of pitting corrosion[17].

4 CONCLUSIONS

1) Al-Mg-Mn-Sc-Zr alloy suffers pitting corrosion in the EXCO solution. During pit incubation, the Nyquist diagram is mainly composed of a depressed capacitive arc at high-mediate frequency and an inductive arc at low frequency. The inductive arc fades with immersion time. The beginning of pitting corrosion and the appearance of two capacitive arcs have simultaneity. So the EIS technique can detect the appearance of pitting-attack of Al-Mg-Mn-Sc-Zr alloy in the EXCO solution, through observing the variations of impedance diagrams.

2) During pit propagation, the specimen surface consists of two parts: a passive surface and a new interface caused by pitting corrosion. The Nyquist diagram is composed of two overlapped capacitive arcs. The capacitive arc at high frequency is aroused by passive surface, and the capacitive arc at low frequency is aroused by the pitting. With the immersion going on, two time constants are more clearly distinguished.

3) The good correspondence between the experiment results and the fitted results is obtained using the equivalent circuit. Every element in the equivalent circuit has distinct physical meaning. The degree and severity of pitting corrosion can be obtained by the features of EIS and comparing the fitted values of parameters at different time.

REFERENCES

[1] YIN Zhi-min, PAN Qing-lin, ZHANG Yong-hong. Effect of trace Sc and Zr on the microstructure and mechanical properties of Al-Mg based alloys [J]. Mater Sci Eng A, 2000, A280: 151-155.

[2] Lathabai S, Lloyd P G. The effect of scandium on the microstructure, mechanical properties and weldability of a cast Al-Mg alloy[J]. Acta Materialia, 2002, 50: 4275-4292.

[3] Roder O, Wirtz T, Gysler A, et al. Fatigue properties of Al-Mg alloys with and without scandium[J]. Mater Sci Eng A, 1997, A234-236: 181-184.

[4] Braun R, Lenczowski B, Tempus G. Effect of thermal exposure on the corrosion properties of an Al-Mg-Sc alloy sheet[J]. Materials Science Forum, 2000, 331-337: 1647-1652.

[5] Wenger F, Cheriet S, Talhi B, et al. Electrochemical impedance of pits: influence of the pit morphology[J]. Corrosion Science, 1997, 39(7): 1239-1252.

[6] Annergren I, Zou F, Thierry D. Application of localised electrochemical techniques to study kinetics of initiation and propagation during pit growth[J]. Electrochimica Acta, 1999, 44: 4383-4393.

[7] LI Di, HU Yang-ling, GUO Bao-lan. Study on the evaluation of localized corrosion of 2024T3 aluminum alloy with EIS[J]. Mater Sci Eng A, 2000, A280: 173-176.

[8] LI Jin-feng, ZHANG Zhao, CAO Fa-he, et al. Investigation of exfoliation corrosion of AA8090 Al-Li alloy using electrochemical impedance spectroscopy [J]. Trans Nonferrous Met Soc China, 2003, 13(2): 320-324.

[9] René Antaño-Lopez, Michel Keddam, Hisasi Takenouti. A new experimental approach to the time-constants of electrochemical impedance: frequency response of the double layer capacitance[J]. Electrochimica Acta, 2001, 46: 3611-3617.

[10] Darowicki K, Krakowiak S, Ślepski P. Evaluation of pitting corrosion by means of dynamic electrochemical impedance spectroscopy [J]. Electrochimica Acta, 2004, 49: 2909-2918.

[11] ASTM. Annual Book of ASTM Standards [S]. ASTM G 66-80, 1986.

[12] Conde A, de Damborenea J. Evaluation of exfoliation susceptibility by means of the electrochemical impedance spectroscopy[J]. Corrosion Science, 2000, 42: 1363-1377.

[13] CAO Chu-nan, WANG Jia, LIN Hai-chao. Effect of Cl^- ion on the impedance of passive-film-covered electrodes[J]. Journal of Chinese Society of Corrosion and Protection, 1989, 9(4): 261-270. (in Chinese)

[14] Keddam M, Kuntz C, Takenouti H, et al. Exfoliation corrosion of aluminium alloys examined by electrode impedance[J]. Electrochimica Acta, 1997, 42 (1): 87-97.

[15] Conde A, de Damborenea J. Electrechemical modeling of exfoliation corrosion behaviour of 8090 alloy [J]. Electrochimica Acta, 1998, 43(8): 849-860.

[16] WANG Jia, CAO chu-nan, LIN Hai-chao. Features of AC impedance of pitting corroded electrodes during pits propagation[J]. Journal of Chinese Society of Corrosion and Protection, 1989, 9(4): 271-279. (in Chinese)

[17] CAI Chao, LI Jin-feng, ZHENG Zi-qiao, et al. Exfoliation corrosion susceptibility of 8090 Al-Li alloy examined by electrochemical impedance spectroscopy [J]. Trans Nonferrous Met Soc China, 2004, 14(4): 742-746.

(Edited by YANG Bing)